Photonic Crystals

DOI: 10.1002/anie.201302311

A Multi-stopband Photonic-Crystal Microchip for High-Performance Metal-Ion Recognition Based on Fluorescent Detection**

Yu Huang, Fengyu Li, Meng Qin, Lei Jiang, and Yanlin Song**

Photonic crystals (PCs), which are dielectric materials with periodic modulation of the refractive index and photonic band-gap properties,[1] have attracted increasing attention in the emerging areas of sensing,[2] catalyst,[3] detection,[4] high-performance optical devices,[5] and other fields.[6] Furthermore, PC detection for ions,[7] DNA,[8] proteins,[9] and other molecules or materials in biological and chemical systems[10] is especially important for fundamental research and potential applications in human health and the environmental pollution.[11] In particular, sensor arrays are a verified valid detection method in the area of multi-analyte testing and high-throughput analysis.[12] Generally, array sensing needs large numbers of serial compounds as sensors to perform the correlative differential analysis. It involves complicated chemical synthesis and valid compound screening. Although many serial sensors have been designed and synthesized,[12–14] it is still a challenge to achieve multi-testing sensor array conveniently and develop general and high-performance multi-analyte detection methods. We have now designed a multi-stopband PC microchip to selectively enhance the sensing fluorescence signal in different channels, and perform a high-efficient multi-analyte discriminant testing. This PC microchip adopts only one simple sensor, 8-hydroxy-quinoline (8-HQ), for the recognition and analysis of 12 various metal ions (Scheme 1). The facile method will be of significance for advanced discriminant analysis of complex analytes in fluorescent sensing systems.

To generate the cross-reactive PC microchip, we carried out the assembly of hydrophilic colloidal particles on a hydrophilic–hydrophobic patterned substrate to construct a PC microchip. Patterned surfaces with different wetting properties have many potential applications, such as microchannels and microreactors,[15] templates for the wettability-driven self-assembly, and the directed growth of thin films.[16] In this case, the hydrophilic–hydrophobic patterned PC microchip was fabricated first by self-assembly of an alkyl phosphonic acid ($CH_3(CH_2)_{17}PO_3H_2$) monolayer (SAM) on a glass substrate, and then ultraviolet light (UV) was used to etch the SAM through a micromask (Supporting Information, Figure S1). Furthermore, the areas with differential wettability show different adsorption from aqueous solution. The aqueous latex synthesized by emulsion polymerization[17] was selectively adsorbed on the hydrophilic areas. Finally, colloidal particles in the latex droplets assembled and formed the PC microchip (Figure 1).

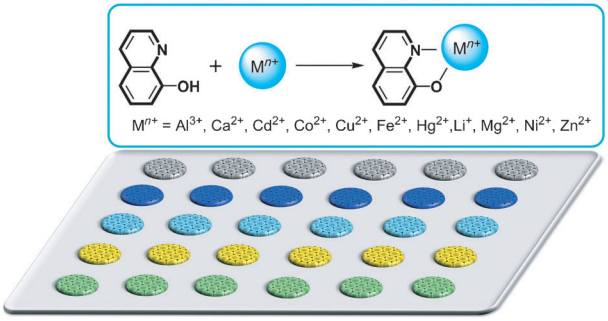

Scheme 1. Multi-analyte discriminant analysis based on 8-HQ with a multi-stopband PC microchip. The colors of pixels indicate the various PCs with different stopbands.

The PC pixels display bright structure colors (Figure 2a), indicating the prominent optical properties of the PC microchip. Figure 2b shows the scanning electron microscope (SEM) image of the PCs, which shows that the colloidal particles are in a face-centered cubic arrangement with a close-packed plane (111) oriented parallel to the substrate. The PCs assembled on the hydrophilic areas of the substrate act as the microchip pixels. In our experiment, the diameter of a dried PC pixel is about 1.0 ± 0.1 mm.

PCs can achieve 20- or even hundred-fold sensitivity enhancement when the stopband matches to the corresponding wavelength of fluorescence.[7–9] However, sensitivity or the limit of detection is just one property for analysis. For the practical complex mixture of samples with multiple analytes or interferents, the recognizability or discriminability is more important. In this study, we fabricated a multi-stopband PC microchip with cross-reactive array to magnify the fluorescence signal in various channels, and improve the discriminability of multi-analyte testing.

8-HQ is well-known as a well-studied metal coordination compound. Its corresponding metalloquinolines display fluo-

[*] Y. Huang, F. Li, M. Qin, L. Jiang, Y. Song
Beijing National Laboratory for Molecular Sciences (BNLMS), Key Laboratory of Green Printing, Key Laboratory of Organic Solids, Institute of Chemistry, Chinese Academy of Sciences
Beijing (P.R. China)
E-mail: ylsong@iccas.ac.cn
forrest@iccas.ac.cn
Homepage: http://ylsong.iccas.ac.cn
Y. Huang, M. Qin
University of the Chinese Academy of Sciences
Beijing (PR China)

[**] F.L. and Y.S. thank the financial support by the National Nature Science Foundation (Grant Nos. 51203166, 51173190, 21074139, 21073203, 91127029, and 21121001) and 973 Program (Nos. 2013CB933004, 2009CB930404, 2011CB932303, and 2011CB808400).

Supporting information for this article is available on the WWW under http://dx.doi.org/10.1002/anie.201302311.

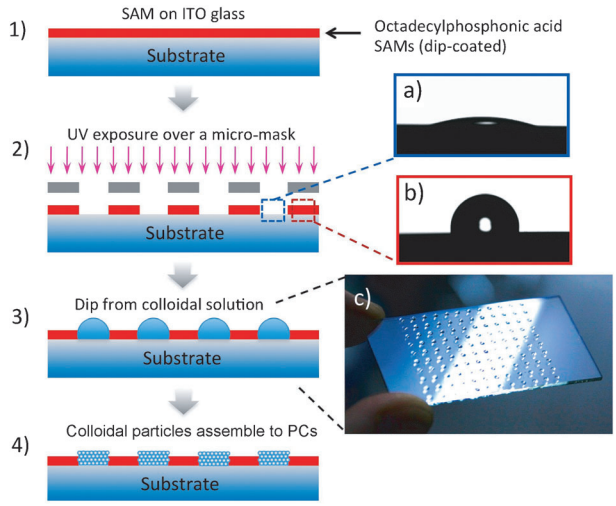

Figure 1. PC microchip fabrication based on a differential wettability patterned substrate. 1) An octadecylphosphonic acid SAM is prepared on an indium tin oxide (ITO) glass; 2) UV light is used to etch the SAM through a micro-mask. The contact angles for areas with or without UV exposure are $17.7 \pm 2.8°$ or $100.9 \pm 3.4°$, respectively. 3) Latex droplets are selectively absorbed on the hydrophilic areas. 4) Colloidal particles are assembled to form the PC microchip.

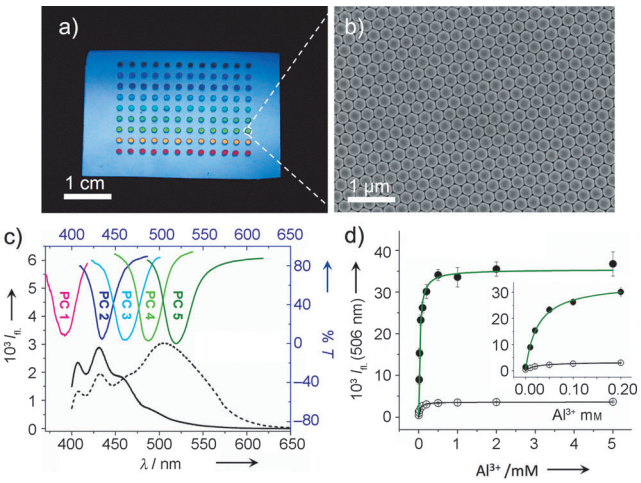

Figure 2. a) A photograph of a multi-stopband PC microchip. b) An SEM image of the PCs. c) Fluorescence spectra of 8-HQ (——) and 8-HQ-Al^{3+} (-----), and transmittance spectra of the PCs. The stopbands of the PCs overlap the different position at three peaks of emission spectra of 8-HQ and 8-HQ-Al^{3+}, respectively. d) The Al^{3+} concentration dependence of the fluorescence at 506 nm on PC 5 (●) and on a blank surface (○). Inset: Detail of the low concentration (0–200 μM) region. The fluorescence intensity on PC 5 shows more than 10 times higher and more-sensitive responses to metal ions than on the blank surface.

rescence modulated by the metal ions, but they hardly yield appreciably differential fluorescence.[18] From chemical modification, such as substitution with extended conjugated fluorescence, 8-HQ fluorescent derivatives can generate a discriminant analysis on the cross-reactive array. However, it involves complicated synthesis and purification processing for six or more serial sensors.[14] Herein, we adopt only the simplest sensor (8-HQ) to realize high-performance multi-analyte testing and discriminant analysis.

Based on fluorescence spectra characteristics of 8-HQ response with metal ions, we designed a microchip combining five PCs with various stopbands, which overlap the whole range of metalloquinoline fluorescence spectra. As Figure 2c shows, we selected PCs with stopbands of 392 nm (PC 1), 434 nm (PC 2), 460 nm (PC 3), 488 nm (PC 4), and 519 nm (PC 5) to overlap the 406 nm, 430 nm and 459 nm and 506 nm of metalloquinoline fluorescence spectra. The PCs on the microchip were assembled by monodisperse poly(St-MMA-AA) (poly(styrene–methyl methacrylate–acrylic acid)) colloidal particles with various diameters of 168 nm (PC 1), 183 nm (PC 2), 193 nm (PC 3), 205 nm (PC 4), and 216 nm (PC 5), respectively (Supporting information, Figures S2, S3). An Al^{3+} concentration-dependence investigation of the fluorescence on PC 5 and blank surface displays the obvious fluorescence enhancing and detection sensitivity improvement of the PCs (Figure 2d; Supporting Information, Figure S4).

We fabricated the microchip containing five rows of PCs (PC 1–5) and one polyurethane (PU) row as the blank. 8-HQ was functionalized into the PC matrix (Supporting Information, Scheme S1) and PU blank pixels. The fluorescence responses of the 8-HQ-PC microchip to the presence of 12 metal ions (Al^{3+}, Ca^{2+}, Cd^{2+}, Co^{2+}, Cr^{3+}, Cu^{2+}, Fe^{2+}, Hg^{2+}, Li^{+}, Mg^{2+}, Ni^{2+}, and Zn^{2+}) were recorded in 6 channels (CH 1: 450 nm, CH 2: 480 nm, CH 3: 505 nm, CH 4: 535 nm, CH 5: 570 nm, CH 6: 605 nm, with UV 365 nm excitation). The fluorescent image of Figure 3a was obtained when the pixels were dried, which shows obvious fluorescence shifts for each PC pixel row. The phenomenon demonstrates the selective fluorescence enhancing of PC stopbands. Figure 3b is

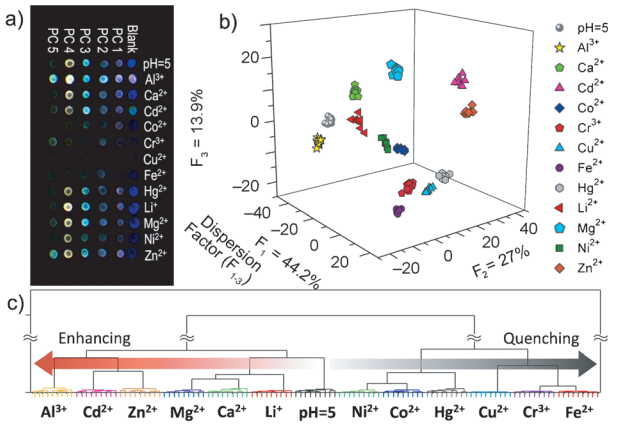

Figure 3. Fluorescence-discriminant analysis of 12 metal ions on a PC microchip, and rational analysis. a) Fluorescence image of a PC microchip spotted by metal ions (1.0 mM in water, 200 nL, pH 5), which was recorded in 6 different channels. The colors were generated by superimposing of the equally weighed images corresponding to RGB channels. b) Graph of the linear discriminant analysis (LDA) showing a clear clustering of the 12 metal ion analytes. The gathering of the clusters demonstrates the good repeatability of the PC microchip for each metal ion response. c) Hierarchical clustering analysis (HCA) gives the similarity clustering of the analytes based on the enhancing or quenching effect of the fluorescence.

a graphic representation of the linear discriminant analysis (LDA) result. The dispersion factors (F_1–F_3) are used to display the discriminative analysis and form the three-dimensional representation of the various analyte clusters. The distance or closeness of the cluster in spatial distribution reveals the large or small differential of fluorescent signal of the metal ions. Meanwhile, the gathering of the clusters into groups demonstrates the good reproducibility of the microchip. The LDA gives the 100% correct classification of the twelve metal ion samples and one control sample, namely water at pH 5 (Supporting Information, Table S1).

An unsupervised multivariate analysis, hierarchical clustering analysis (HCA), performs dimensionality reduction analysis to investigate the similarity clustering of the analytes. In Figure 3c, HCA graphical output shows two major and four minor groups, which indicates analyte-specific quenching-enhancement and absorption-emission shifts that are due to the electropositivity of various metals.[14] The rational analysis demonstrates that the fluorescence enhancement of the PC microchip reflects the original information of sensing and indicates more subtle and accurate details (Supporting Information, Figures S5–S7).

To evaluate classification efficiency and to magnify the effect of PCs with various stopbands, we explored the LDA of PCs 1–5 or PU array separately (Supporting Information, Tables S2–S7). As presented in Table S9, none of the PC array can result in the completely correct classification individually. The PCs with a blue band edge of the stopbands matching the major fluorescence characteristic peak of metalloquinoline (430 nm matching of PC 2 and 506 nm matching of PC 5) can result the higher correct classification (88% for PC 2 array, 89% for PC 5 array). It comes from a high-density slow-photon effect.[19] The lower correct classification of PC 1 (76%) and PC 4 (75%) are the result of the low-density slow photon of the red band edge overlapping. Interestingly, the PC 3 array (56%) performs an even poorer correct classification than the blank array (62%). The unconventional phenomenon is due to the PC 3 stopband overlapping at 460 nm, a singularity on metalloquinoline fluorescence spectra, which is the minimum change position of sensing. The sameness enhancing dilutes the difference enhancing, and leads to a negative action in the discriminant analysis.

Although the more information usually results the clearer discriminant analysis, not every data element makes the positive contribution. Upon the evaluation analysis of the PC efficiency, we used two PCs (PC 2 and PC 5) with the highest classification to combine a new 8-HQ-PC microchip. It still results in a 100% completely correct classification LDA of the 12 metal ions and one control sample (Supporting Information, Figure S8 and Table S11). With rational design, the multi-stopband PC microchip can perform multi-analyte pattern recognition with high efficiency.

In summary, to achieve general and high-performance multi-analyte discriminant testing, we designed and fabricated a multi-stopband PC microchip based on hydrophilic–hydrophobic patterned substrate. The microchip can selectively enhance the sensing fluorescence in different channels, and perform a high-efficient multi-analyte discriminant testing. It is remarkable that just one simple sensor, 8-HQ, facilitates the recognition and analysis of 12 different metal ions. The efficiency evaluation of discriminant analysis improves the PC microchip efficiency from five to just two PCs. The facile fabrication of a high-performance PC microchip and the insight of sensing efficiency evaluation will be of great importance for the development of advanced discriminant analysis for complex analytes in fluorescent sensing systems and devices.

Received: March 19, 2013
Revised: April 18, 2013
Published online: June 10, 2013

Keywords: metal ions · multi-analyte recognition · patterned substrates · photonic crystals · sensor-array microchips

[1] a) E. Yablonovitch, *Phys. Rev. Lett.* **1987**, *58*, 2059–2062; b) S. John, *Phys. Rev. Lett.* **1987**, *58*, 2486–2489.
[2] a) J. H. Holtz, S. A. Asher, *Nature* **1997**, *389*, 829–832; b) M. Xu, A. V. Goponenko, S. A. Asher, *J. Am. Chem. Soc.* **2008**, *130*, 3113–3119; c) J. P. Ge, H. Lee, L. He, J. Kim, Z. D. Lu, H. Kim, J. Goebl, S. Kwon, Y. D. Yin, *J. Am. Chem. Soc.* **2009**, *131*, 15687–15694.
[3] J. I. L. Chen, G. von Freymann, S. Y. Choi, V. Kitaev, G. A. Ozin, *Adv. Mater.* **2006**, *18*, 1915–1919.
[4] I. B. Burgess, L. Mishchenko, B. D. Hatton, M. Kolle, M. Loncar, J. Aizenberg, *J. Am. Chem. Soc.* **2011**, *133*, 12430–12432.
[5] a) A. Mihi, C. J. Zhang, P. V. Braun, *Angew. Chem.* **2011**, *123*, 5830–5833; *Angew. Chem. Int. Ed.* **2011**, *50*, 5712–5715; b) Y. Huang, J. M. Zhou, B. Su, L. Shi, J. X. Wang, S. R. Chen, L. B. Wang, J. Zi, Y. L. Song, L. Jiang, *J. Am. Chem. Soc.* **2012**, *134*, 17053–17058.
[6] a) J. P. Ge, Y. D. Yin, *Angew. Chem.* **2011**, *123*, 1530–1561; *Angew. Chem. Int. Ed.* **2011**, *50*, 1492–1522; b) O. Sato, S. Kubo, Z. Z. Gu, *Acc. Chem. Res.* **2009**, *42*, 1–10; c) J. X. Wang, Y. Z. Zhang, S. T. Wang, Y. L. Song, L. Jiang, *Acc. Chem. Res.* **2011**, *44*, 405–415.
[7] L. Y. Cui, W. Shi, J. X. Wang, Y. L. Song, H. M. Ma, L. Jiang, *Anal. Methods* **2010**, *2*, 448–450.
[8] M. Z. Li, F. He, Q. Liao, J. Liu, L. Xu, L. Jiang, Y. L. Song, S. Wang, D. B. Zhu, *Angew. Chem.* **2008**, *120*, 7368–7372; *Angew. Chem. Int. Ed.* **2008**, *47*, 7258–7262.
[9] W. Z. Shen, M. Z. Li, L. A. Xu, S. T. Wang, L. Jiang, Y. L. Song, D. B. Zhu, *Biosens. Bioelectron.* **2011**, *26*, 2165–2170.
[10] a) Y. J. Zhao, X. W. Zhao, J. Hu, J. Li, W. Y. Xu, Z. Z. Gu, *Angew. Chem.* **2009**, *121*, 7486–7488; *Angew. Chem. Int. Ed.* **2009**, *48*, 7350–7352; b) Y. J. Zhao, X. W. Zhao, Z. Z. Gu, *Adv. Funct. Mater.* **2010**, *20*, 2970–2988.
[11] a) N. D. Shapiro, S. Soh, K. A. Mirica, G. M. Whitesides, *Anal. Chem.* **2012**, *84*, 6166–6172; b) R. H. Perry, M. Splendore, A. Chien, N. K. Davis, R. N. Zare, *Angew. Chem.* **2011**, *123*, 264–268; *Angew. Chem. Int. Ed.* **2011**, *50*, 250–254; c) A. R. Wheeler, W. R. Throndset, R. J. Whelan, A. M. Leach, R. N. Zare, T. H. Liao, K. Farrell, I. D. Manger, A. Daridon, *Anal. Chem.* **2003**, *75*, 3581–3586; d) Y. J. Yang, B. Szamosfalvi, J. Yee, S. Frinak, E. V. Anslyn, *Analyst* **2011**, *136*, 317–320; e) Y. J. Yang, S. K. Seidlits, M. M. Adams, V. M. Lynch, C. E. Schmidt, E. V. Anslyn, J. B. Shear, *J. Am. Chem. Soc.* **2010**, *132*, 13114–13116.
[12] a) J. J. Lavigne, E. V. Anslyn, *Angew. Chem.* **2001**, *113*, 3212–3225; *Angew. Chem. Int. Ed.* **2001**, *40*, 3118–3130; b) P. Anzenbacher, F. Y. Li, M. A. Palacios, *Angew. Chem.* **2012**, *124*, 2395–2398; *Angew. Chem. Int. Ed.* **2012**, *51*, 2345–2348;

c) B. Rout, L. Unger, G. Armony, M. A. Iron, D. Margulies, *Angew. Chem.* **2012**, *124*, 12645 – 12649; *Angew. Chem. Int. Ed.* **2012**, *51*, 12477 – 12481.
[13] a) J. Kim, X. Q. Wu, M. R. Herman, J. S. Dordick, *Anal. Chim. Acta* **1998**, *370*, 251 – 258; b) J. Tan, H. F. Wang, X. P. Yan, *Biosens. Bioelectron.* **2009**, *24*, 3316 – 3321.
[14] a) M. A. Palacios, Z. Wang, V. A. Montes, G. V. Zyryanov, P. Anzenbacher, *J. Am. Chem. Soc.* **2008**, *130*, 10307 – 10314; b) Z. Wang, M. A. Palacios, P. Anzenbacher, *Anal. Chem.* **2008**, *80*, 7451 – 7459.
[15] a) H. Gau, S. Herminghaus, P. Lenz, R. Lipowsky, *Science* **1999**, *283*, 46 – 49; b) B. Zhao, J. S. Moore, D. J. Beebe, *Science* **2001**, *291*, 1023 – 1026.
[16] a) L. D. Zarzar, P. Kim, M. Kolle, C. J. Brinker, J. Aizenberg, B. Kaehr, *Angew. Chem.* **2011**, *123*, 9528 – 9532; *Angew. Chem. Int. Ed.* **2011**, *50*, 9356 – 9360; b) T. S. Wong, S. H. Kang, S. K. Y. Tang, E. J. Smythe, B. D. Hatton, A. Grinthal, J. Aizenberg, *Nature* **2011**, *477*, 443 – 447; c) T. L. Sun, G. Y. Qing, B. L. Su, L. Jiang, *Chem. Soc. Rev.* **2011**, *40*, 2909 – 2921; d) T. L. Sun, G. J. Wang, L. Feng, B. Q. Liu, Y. M. Ma, L. Jiang, D. B. Zhu, *Angew. Chem.* **2004**, *116*, 361 – 364; *Angew. Chem. Int. Ed.* **2004**, *43*, 357 – 360.
[17] J. X. Wang, Y. Q. Wen, H. L. Ge, Z. W. Sun, Y. M. Zheng, Y. L. Song, L. Jiang, *Macromol. Chem. Phys.* **2006**, *207*, 596 – 604.
[18] E. Bardez, I. Devol, B. Larrey, B. Valeur, *J. Phys. Chem. B* **1997**, *101*, 7786 – 7793.
[19] a) J. I. L. Chen, G. von Freymann, S. Y. Choi, V. Kitaev, G. A. Ozin, *J. Mater. Chem.* **2008**, *18*, 369 – 373; b) J. Li, X. W. Zhao, Y. J. Zhao, J. Hu, M. Xu, Z. Z. Gu, *J. Mater. Chem.* **2009**, *19*, 6492 – 6497; c) G. R. Maskaly, M. A. Petruska, J. Nanda, I. V. Bezel, R. D. Schaller, H. Htoon, J. M. Pietryga, V. I. Klimov, *Adv. Mater.* **2006**, *18*, 343 – 347.

